

## A site-specific land and water management model in MIKE SHE

M.H. Rubarenzya<sup>1\*</sup>, D. Graham<sup>2</sup>, J. Feyen<sup>3</sup>, P. Willems<sup>1</sup> and J. Berlamont<sup>1</sup>

<sup>1</sup>Department of Civil Engineering, Katholieke Universiteit Leuven, Kasteelpark Arenberg 40, B-3001 Heverlee, Belgium. \*Corresponding author. E-mail: [MarkHenry.Rubarenzya@bwk.kuleuven.be](mailto:MarkHenry.Rubarenzya@bwk.kuleuven.be)

<sup>2</sup>DHI Water & Environment, Agern Allé 5, DK-2970 Hørsholm, Denmark

<sup>3</sup>Department of Land Management and Economics, Katholieke Universiteit Leuven, B-3001 Heverlee, Belgium

**Abstract** This paper presents the development and characteristics of a site-specific physically based, spatially distributed model. The Grote Nete catchment model was built to simulate the various processes of the hydrological cycle, and their interactions with each other. It highlights the various stages of model development from conceptualisation and the underlying mathematical representation of hydrological processes, through the model set-up phase, and finally to the calibration and validation. MIKE SHE was chosen for its ability to generate a spatially distributed representation of the hydrological processes within a catchment, which was necessary for future scenario analysis. The equations coupled within the system include a three-dimensional Darcy equation in the saturated zone, the Richards equation for the unsaturated zone, the diffusion wave equation for areal overland flow and the fully dynamic Saint Venant equations for flow in channels. Evapotranspiration from the surface and subsurface are modelled using land cover and climatic factors to define the complete water budget using a physically based formulation. The paper presents the results of a multi-criteria evaluation protocol that included graphical and statistical testing, which involved the use of seven data comparison plots. Results of model calibration and validation against pre-established criteria are presented and discussed.

**Keywords** Distributed modelling; Grote Nete; MIKE SHE; site-specific model

### Introduction

In Flanders, as in much of Belgium, water resources have been profoundly influenced by anthropogenic activities, including the construction of canals, agricultural and land drainage systems, and land use changes. Physical deterioration of rivers and their floodplains is common. Less than 20% of the rivers are still in a natural physical state. Engineering works have significantly changed water retention capacity, among other river characteristics, and this appears to be resulting in increasing incidences of extreme hydrological events. Awareness and concern have increasingly been directed towards the potential adverse impacts that anthropogenic changes have had on river valley ecosystems. Scientists have come to realize that mankind's economic strides made over the last two centuries were at the expense of the Earth's biodiversity, its environment and the stability of its self-regulatory systems (Todd *et al.* 2003). Almost no stream or river has been left in its natural state (Ripl *et al.* 1995). The growing awareness of the value of natural ecosystems has resulted in various efforts being initialized to reverse past anthropogenic changes (Jungwirth *et al.* 2002; Pedroli *et al.* 2002; Palmer *et al.* 2005). This stance, in essence, represents a shift from the past practice of taming rivers and conquering river valleys, towards an emerging trend of restoration and conservation. However, the reinstatement of a balance between mankind and nature could involve reduction of the negative human footprint on the Earth by up to 90% (Todd *et al.* 2003). Various methods for natural restoration are being considered.

Quantitative and qualitative information on these intervention measures are known to fluctuate with country or region, extent of ecological degradation, present land use within the region and understanding of the accompanying hydrological processes (Kusler and Kentula 1990; Richardson 1994; Mitsch and Wilson 1996). The focus of this science is on the quest for sustainable ecosystems in which human and natural values are in harmony (Mitsch 1993, 1998; Mitsch *et al.* 2002). In Flanders efforts to reverse the trend of ecosystem degradation have led to river valley rewetting being considered by water managers. River valley rewetting involves increasing the water contained in the river valley through one of two processes, namely groundwater and surface water rewetting. It can be achieved by any of several methods including: restoring upstream infiltration; reduction of parcel drainage; reduction of groundwater abstraction; reduction of basin level drainage by re-meandering, allowing for macrophyte vegetation growth, reduction of depth–width ratio or pinching; diverting surface water into riparian wetland and (artificial) side channels; allowing water to reside in riparian depressions after flooding (river bank overflow); or by dike and weir level regulation. It is believed to influence the ecology positively, especially during the dry summer months.

However, the hydrological influence river valley rewetting on the catchment over the annual cycle remains unclear. In regions like Belgium, this is especially with regard to a potential for increased flooding during the wet winter months. In addition, changing people's views on water use and making them understand the meaning and necessity of good watershed management requires solid scientific arguments. Such arguments can be communicated to the stakeholders involved through the use of examples and models. Models are used to answer the research questions that arise with water retention, including the risks associated with water conservation, the required extent of basin restoration and the existence of other options to address the primary problem of hydrological extremes. Scenarios are used as a prerequisite for assessing the influence of potential land use/land cover changes on runoff generation (Niehoff *et al.* 2002). Thus, to fill the existing gap in knowledge of the hydrological influence of river valley rewetting and provide a basis for undertaking watershed management with stakeholders, it was necessary to develop a physically based, spatially distributed model in which the overland and channel flow processes were defined, as indeed were the surface/subsurface interactions which include depression storage as a physical process influencing water flow over the ground. The distributed hydrological model would assign both spatial and temporal representation to the area under study. The method is based on the blueprint of Freeze and Harlan (Beven 2001), and has not evolved much in time. Its main promise lies in the promise for scenario generation where no calibration information is possible (Beven 1985, 2001; Smith *et al.* 1994). The technique offers the best approximation of physical reality, especially when physically based parameter sets are used for the models. Also included was a coupled river network model. Channel roughness was represented by Manning's roughness, while the interaction between the channel and the underlying bed and aquifer was defined through a leakage coefficient. Evapotranspiration was calculated on the basis of empirical equations that described the plant interception, transpiration and soil evaporation. All processes were fully coupled and interacted with each other.

Problems involving strong interactions between surface-water and groundwater regimes, as well as investigations of conjunctive water management issues, necessitate coupled simulation of the surface and subsurface flow regimes. Characterisation of flow processes individually within these regimes is well established. Attempts have also been made to link (via time-lagging or iterative coupling) some or all of these flow regimes to analyse more complete flow behaviour. MIKE SHE (Graham and Butts 2006) offers one such example of linking of subsurface, overland and channel flow processes for determining the general

response of a watershed due to interactions among individual processes. While a site-specific model is able to adequately represent discharge from the catchment, distributed hydrological modelling is not without its limitations. These are primarily due to scale, nonlinearity, uniqueness, equifinality and uncertainty (Beven 2001). Hydrological systems are nonlinear (Reggiani *et al.* 1998, 1999, 2000). Their theorising and modelling are held back by the absence of a scale theory (Blöschl 2001). Most models are not transferable, but are best suited to the conditions under which they were developed. Equifinality (Beven 1993, 1996) recognises that there are several model structures and parameter sets that will acceptably simulate the available data. And, finally, uncertainty recognises the limitations and uncertainties in model structure and parameter estimation or measurement.

The paper presents the application of MIKE SHE to the Grote Nete catchment in Belgium. It gives insights into how this general code was adapted to represent the local hydrology through, among other measures, a simplification of some of the equations governing basic hydrological processes. The objective here was to develop a useful physically based, fully distributed model of the Grote Nete catchment. Such a model would then be used to study the hydrological influence of river valley rewetting and, in so doing, contribute to a better understanding of the hydrological effects of catchment rewetting.

## Methods and materials

### The Grote Nete catchment

The Grote Nete catchment is a middle-sized hydrological catchment located in the northeast of Flanders (Figure 1). It is predominantly composed of sandy loam to sandy soils, and has a shallow water table. Average precipitation in the area ranges from 743 to 800 mm/yr. The topography is flat, ranging from 12 m in the west to 69 m in the east with an average value of 22 m (Batelaan 2006). The catchment is drained by the Grote Nete, Molse Nete and Grote Laak Rivers and their tributaries, and includes a dense network of agricultural drains. The Grote Nete River originates at the foot of the north-western edge of the Campine plateau. The basin area of the outlet limnigraphic station at Varendonk is 385 km<sup>2</sup>. The catchment has two important limnigraphic stations namely, Vorst (AMINAL 992/2) on the Grote Laak and Varendonk (AMINAL 994) on the Grote Nete (VLIZ: Flanders Marine Institute 2006). Both stations have hourly discharge data series, which were used during model development.

### Modelling environment

*Physically based, fully distributed model, MIKE SHE.* In deciding upon which model to use in this research, it was recognised that an appropriate model may be difficult to choose, and models simulating with similar data can produce very different responses (Michaud and Sorooshian 1994; Refsgaard and Knudsen 1996; Carpenter and Georgakakos 2004;

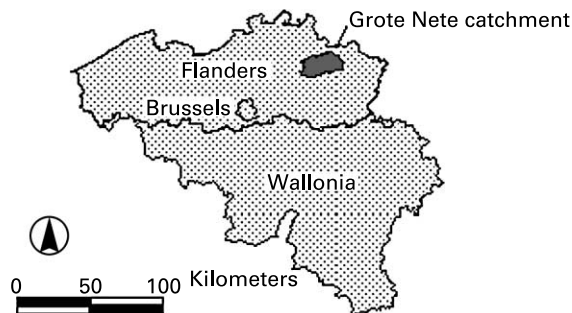


**Figure 1** Map of Belgium showing the three main political regions, and the location of the study area in grey

Reed *et al.* 2004). However, an important consideration here was the applicability of the model for scenario analysis, which necessitated the generation of a spatially distributed representation of the hydrological processes within the study area. MIKE SHE (Refsgaard and Storm 1995) was selected for hydrological modelling. It is a dynamic modelling tool that simulates the entire land phase of the hydrologic cycle. It includes all of the processes in the land phase of the hydrologic cycle (including precipitation, evapotranspiration, canopy interception, overland sheet flow, channel flow, unsaturated subsurface flow and saturated groundwater flow (Figure 2). The hydrodynamic module, MIKE 11 (Havno *et al.* 1995), provides a library of computational methods for steady and unsteady flow in channel networks as well as quasi-two-dimensional flow simulation on flood plains. The fully dynamic wave approximation of the Saint-Venant equations was solved numerically between all grid points at specified time intervals for given boundary conditions.

*Time series analysis tool, WETSPRO.* Water Engineering Time Series PROcessing tool (WETSPRO) (Willems 2000), a tool for time series analysis, was used to perform an analysis of the river discharge series at Varendonk and Vorst limnigraphic stations. A recursive digital filter for exponential recessions was used to split total rainfall–runoff discharges into its three component sub-flows (base flow, interflow and overland flow) using the recession constants for each component. This was done by means of a numerical digital filter, whose concept of recession time is derived from that of a linear reservoir. The equations governing the recursive digital filter for exponential recessions are a generalisation of those derived by Chapman (Willems 2003). This generalisation introduced two new parameters,  $\nu$  and  $\omega$ , where  $\omega$  is the fraction of the cumulative values in the total time series that is related to the filtered component of flow, and  $\nu$  is defined as

$$\nu = (1 - \omega)/\omega \quad (1)$$

$$f(t) = af(t - 1) + b(q(t) - \alpha q(t - 1)) \quad (2)$$

$$b(t) = \alpha b(t - 1) + c(1 - \alpha)(f(t - 1) + f(t)) \quad (3)$$

and for the above relationships,

$a = ((2 + \nu)\alpha - \nu)/(2 + \nu - \nu\alpha)$ ;  $b = (2/(2 + \nu - \nu\alpha))$ ;  $c = 0.5\nu$ ;  $q(t)$  represents the combined discharge;  $b(t)$  represents the time series of the filtered component with recession constant  $k$ ;  $t$  represents time; and  $f(t)$  represents the higher frequency components.

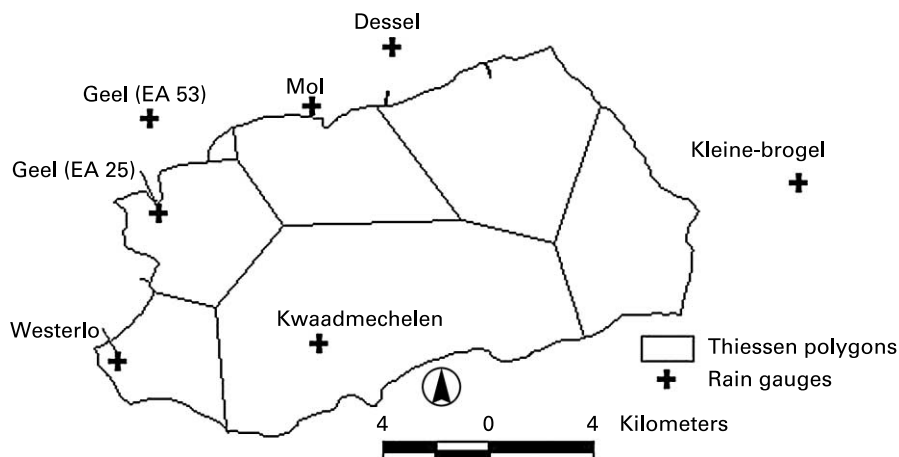


**Figure 2** The study area showing rainfall gauging stations and their corresponding Thiessen polygons

The flow separation was based upon the significantly different recession constants of the flow components, and calibration of the recession constant was done visually. Results of this component flow filtration of the river discharge are shown in [Table 1](#).

#### Model input analysis

*Rainfall measurements.* Spatially distributed rainfall input was used. This input was derived from rainfall data of seven gauging stations ([Figure 3](#)) in and close to the catchment. An analysis of the rainfall records revealed that gaps were present in four of the seven records ([Rouhani 2004](#)). Periods of missing data in individual stations were filled with data obtained from the closest station for which such data was available. This was done after it was determined that the records from the different stations were quite homogeneous ([Figure 3](#)) and without significant spatial variability, and a previous study by Willems ([Willems et al. 2002](#)) had established that there are no micro-climatic effects over the Grote Nete catchment. During the process of filling in missing data, differences in average rainfall volumes for different stations were addressed by use of the “normal-ratio method” of gap filling. A correction factor was applied to the rainfall data from the closest stations before this data could be used in the estimation of the missing rainfall values. The correction factor was defined as

$$r = (R/R_C)r_C \quad (4)$$

where  $r$  denoted the computed daily rainfall during a missing period,  $R$  denoted the long term average rainfall at the station with missing data,  $R_C$  denoted the long term average rainfall at the closest station and  $r_C$  denoted the observed daily rainfall at the closest station.

*Potential evapotranspiration.* The potential evapotranspiration,  $E_p$ , was calculated for a closed, short cut grass surface, optimally supplied with water, and using coefficients that were calibrated for Belgian conditions. In estimating the evapotranspiration,  $ET_o$ , climatic data from the meteorological station at Geel ( $51^\circ 09'30''$  N,  $4^\circ 59'30''$  E; at elevation 21 m) was used. This data included relative humidity (%), minimum and maximum temperature ( $^\circ\text{C}$ ), solar radiation ( $\text{J cm}^{-2} \text{d}^{-1}$ ), number of sunshine hours and wind velocity at 2 m above ground level ( $\text{m}^2/\text{s}$ ). The Penman–Monteith FAO-56 method was used for the calculation of the  $ET_o$  data set ([Vazquez 2004](#); [Allen et al. 1998](#)), using the ETREF software ([Raes et al. 1986](#)).

#### Modelling of the water cycle

What follows is a description of the relationships and equations used in representing the water (hydrological) cycle for the site-specific Grote Nete catchment model and, where appropriate, explanations for why certain formulations were used. A rigorous approach satisfying flow continuity in three dimensions in both the saturated and unsaturated zones of the subsurface is required for robust and reliable solutions for subsurface flow under a variety

**Table 1** WETSPRO filter output on measured discharges at the limnigraphic stations. The values indicate the filtered components of discharge as percentages of the total discharge

	Period	Baseflow (%)	Interflow (%)	Overland flow (%)	Total (%)
Varendonk	Calibration	72	15	13	100
	Validation	77	12	11	100
Vorst	Calibration	77	11	12	100
	Validation	77	11	12	100

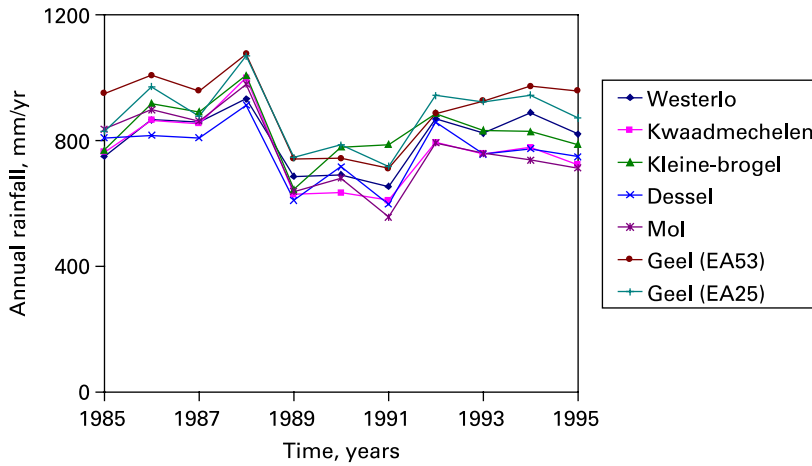


**Figure 3** Trend of annual rainfall for the seven rainfall stations in and close to the Grote Nete catchment that were used in model development

of general flow conditions. This was provided by the mixed form of Richard’s equation for variably saturated subsurface flow subject to evapotranspiration and various other boundary conditions. **Figure 4** shows the relationships between the different hydrological processes. The figure illustrates the distinction between processes that had one-way flow as opposed to those that proceeded in both directions. It is worth pointing out that all these interactions, as

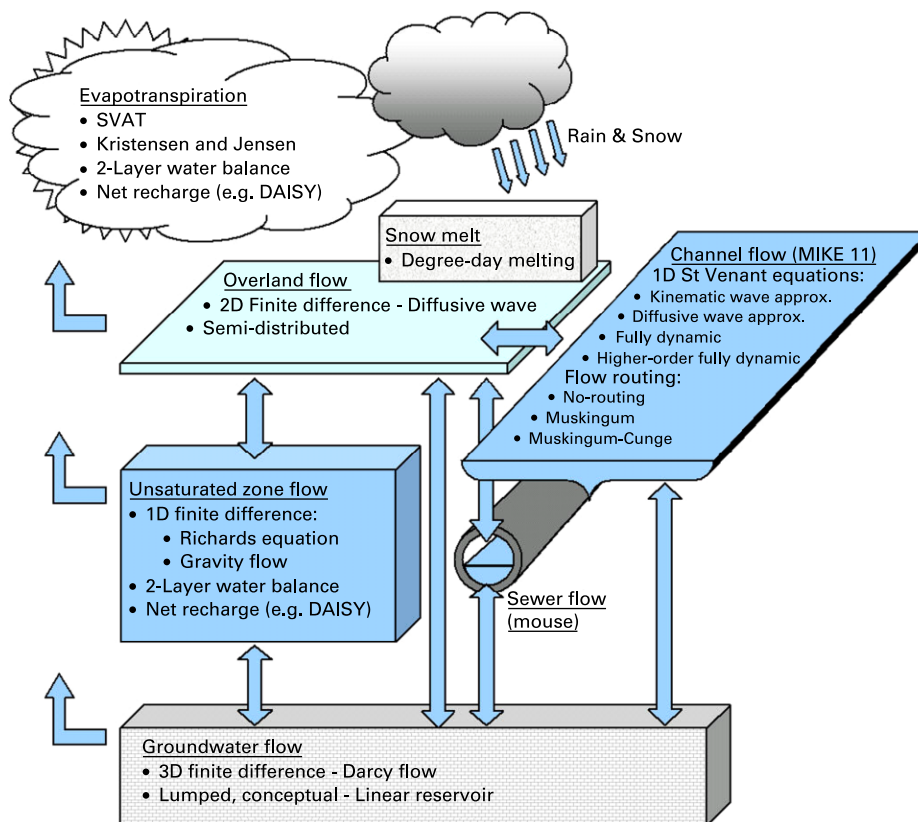


**Figure 4** Interaction of modules in MIKE SHE

represented by arrows, were being modelled simultaneously. The processes were dynamic in nature. Each of these processes was represented at different levels of spatial distribution and complexity, dependent upon the availability of field data.

*Saturated zone flow.* The saturated zone model consisted of a three-dimensional Darcy equation. This permitted three-dimensional flow in the heterogeneous aquifer with shifting conditions between unconfined and confined conditions. The spatial and temporal variations of the dependent variable (the hydraulic head) were described mathematically within the equation, which was solved numerically by an iterative implicit finite difference technique:

$$\frac{\partial}{\partial x} \left( K_x \frac{\partial h}{\partial x} \right) + \frac{\partial}{\partial y} \left( K_y \frac{\partial h}{\partial y} \right) + \frac{\partial}{\partial z} \left( K_z \frac{\partial h}{\partial z} \right) - Q = S \frac{\partial h}{\partial t} \quad (5)$$

where,  $K_x$ ,  $K_y$ ,  $K_z$  represent hydraulic conductivity along the  $x$ ,  $y$  and  $z$  axes,  $h$  represents the hydraulic head,  $S$  represents the specific storage coefficient and  $Q$  represents the source/sink terms. The flow was calculated using a maximum allowable time step of 1 h.

*Hydrogeological parameters.* The catchment geology was described in terms of four geological layers to which hydraulic properties were assigned through grid-code files. The three-dimensional geological model described the extent, thicknesses and elevation of the layers. For each layer, distributed estimates were determined for the horizontal and vertical hydraulic conductivities. Calibrated parameter values for the specific yields and storage coefficients are given in [Table 2](#).

*Groundwater abstraction.* A separate well file was created to represent the abstraction from the five abstraction wells located within the catchment, and another three just outside the boundary. Included in this file were the coordinates of each well, the vertical location of the filter and a time series of water abstraction.

*Drainage.* The drainage component of the MIKE SHE groundwater module was included. It described drainage using drainage codes (areas considered to be drained), drain levels (distributed maps of effective drainage levels, i.e. groundwater table elevation above which drainage flow occurs) and a drainage time constant. Drained water was routed to rivers based on the grid codes. The calibrated model had a drainage time constant of  $7 \times 10^{-7} \text{ s}^{-1}$ . It was not feasible to measure the drainage levels directly in the field. A value of 1 m was used, which is believed to be the average depth to the phreatic surface.

*Vadose zone flow.* The unsaturated zone model was a vertical soil profile model that interacted with both the overland flow and the groundwater model. The lower boundary condition for this zone was defined by the location of the groundwater table. The Richards Equation (Equation (6)) was used to represent flow in this zone:

**Table 2** Hydrogeological parameters for the Grote Nete model

	Specific yield	Storage coefficient (1/m)
Layer 1	0.30	0.0001
Layer 2	0.35	0.0005
Layer 3	0.25	0.0001
Layer 4	0.25	0.0001

$$C \frac{\partial \psi}{\partial t} = \frac{\partial}{\partial z} \left( K \frac{\partial \psi}{\partial z} \right) + \frac{\partial K}{\partial z} - S \quad (6)$$

where  $C = \partial \theta / \partial \psi$  is the soil water capacity.

A particular module, the gravity flow module, was adopted for the study area given the raised water table in the area (on average 1 m below the ground surface) (Rubarenzya et al. 2005a; Graham and Butts 2006). The driving force for transport of water in the unsaturated zone is the gradient of the hydraulic head,  $h$ , composed of a gravitational component,  $z$ , and a pressure component,  $\psi$ :

$$h = z + \psi \quad (7)$$

The gravitational head at a point is the elevation of the point above the datum ( $z$  is positive upwards). The reference level for the pressure head component is atmospheric pressure. Under unsaturated conditions the pressure head,  $\psi$ , is negative due to capillary forces and short range adsorptive forces between the water molecules and the soil matrix. However, in the gravity flow module, the pressure head term is ignored and the driving force is due entirely to gravity. Thus, for vertical flow, the vertical gradient of the hydraulic head becomes 1. The unit gradient assumed in the gravity flow model means that the gradient is not influenced by capillarity and thus is ignored. This eliminates the nonlinearity associated with the soil moisture–pressure relationship and results in faster calculation of the infiltration. This makes no difference in terms of evapotranspiration except in the event that the water table is beneath the root zone, but close enough to the root zone such that the capillary rise reaches the root zone. In this case, the roots that reach the capillary zone can extract water from the saturated zone – and this is only necessary if the soil is dry and the plants cannot extract any more water from the unsaturated zone. However, given that the groundwater table in the Grote Nete catchment is shallow, the use of the gravity flow module is backed by the reasonable assumption that the plant roots will generally be able to draw water from the saturated zone. Following this,

$$q = -K(\theta) \frac{\partial h}{\partial z} = -K(\theta) \quad (8)$$

where  $q$  is the volumetric flux as obtained from Darcy's law.

Assuming an incompressible soil matrix and constant soil water density, the continuity equation for gravity flow became

$$\frac{\partial \theta}{\partial t} = - \frac{\partial q}{\partial z} - S(z) \quad (9)$$

where  $\theta$  is the volumetric soil moisture,  $K(\theta)$  is the saturated hydraulic conductivity and  $S$  denoted the root extraction sink term.

*Soil characteristics and properties.* The study area is characterised by sandy to sandy loam soils, and has a high water table. The distributed soil map was broadly classified into six major classes namely podzols, c-development, open water, dunes, alluvial soils and anthropogenic soils. Vertical discretisation then followed from the ground surface down to 20 m. The minimum discretised cell height was 0.025 m at the ground surface. To each discretised layer, soil properties were assigned, including the retention curve parameters and Averjanov pedotransfer coefficients (Rubarenzya et al. 2006). Vertical flow and water content of the unsaturated soil was calculated using a maximum time step of 30 min. MIKE SHE automatically updated the computational time steps during the simulation to avoid numerical instability following high rainfall inputs.



*Overland flow.* The overland flow component was defined by the two-dimensional diffusion wave approximation of the Saint Venant equations governing shallow water flow. For a depth of flow,  $h$ , and flow components  $u$  and  $v$  in the  $x$  and  $y$  directions of a rectangular Cartesian coordinate grid, the diffusion wave approximation of the Saint Venant equations was obtained by ignoring momentum losses that resulted from local and convective acceleration, and lateral inflows perpendicular to the flow direction. To limit the amount of water that could flow over the ground, a parameter for water detention was introduced. Detention storage of 2 mm was applied to the final model, which implied that the depth of water on the surface would have to be more than this value before it could commence flowing as overland flow. However, the model was not very sensitive to this parameter. The overland flow was calculated using a maximum time step of 30 min. An initial water depth of 0 m was used. The distributed surface roughness over the catchment was established after calibration of values from the literature.

*Channel flow and surface water features.* The Grote Nete catchment is composed of numerous river tributaries. In addition, the catchment has many small lakes, the result of sand mining in the past for glass production. Surface waters were represented as land use categories, along with the corresponding roughness and evapotranspirative parameters. The river network was represented in MIKE 11, which is a hydrodynamic model that is coupled to MIKE SHE and simulates the one-dimensional river flows and water levels using the fully dynamic Saint Venant equations. The equations can be written in the form (Tucciarelli 2003)

$$\frac{\partial \sigma}{\partial t} + \frac{\partial q}{\partial x} = Q \quad (10)$$

and

$$\frac{\partial q}{\partial t} + \frac{\partial}{\partial x} \left( \frac{q^2}{\sigma} \right) + g\sigma \frac{\partial H}{\partial x} + \frac{gn^2 q^2}{\sigma \mathfrak{R}^{4/3}} = 0 \quad (11)$$

where  $\sigma$  represents the flow section,  $q$  represents the river discharge,  $h$  represents the water depth,  $n$  represents Manning's coefficient,  $H$  represents the water depth plus bed elevation (total water level),  $\mathfrak{R}$  represents the hydraulic radius and  $Q$  represents the entry discharge per unit length.

The rivers were approximated by the sides of the grid cells in MIKE SHE. The model had a total of 245  $h$  points and 210  $Q$  points (head and discharge points, respectively). Boundary conditions were specified at upstream and downstream ends of the river network. The maximum discretisation was 750 m distance ( $dx$ ), with a fixed time step ( $dt$ ) of 10 min. Rivers and tributaries within the catchment are unlined: therefore, in modelling the exchange flow between the river and the underlying aquifer, the resistance was assumed to be from the aquifer material only.

*Interception and evapotranspiration.* The Kristensen–Jensen model (Kristensen and Jensen 1975) was used to represent evapotranspiration. In applying this model, the net rainfall was first calculated from the total rainfall by subtracting water intercepted by the leaves. The retention of precipitation on the leaves, branches and stems of vegetation was modelled. The interception process was simulated such that precipitation in excess of interception storage and evaporation from interception was able to reach the ground surface. This was computed at the start of every time step of simulation at each model spatial location. The interception storage varied between zero and the interception storage capacity,  $I_{\max}$ , whose value was dependent upon the vegetation type and its stage of development. Evapotranspiration was first removed from intercepted rainfall, and then from ponded water at the reference evapotranspiration rate. The actual soil

moisture content, soil field capacity and wilting point in each vertical cell were used to control the amount of transpiration.

*Land use and vegetation.* The final land use map was based on the 1995 land use map of Flanders. However, the latter map had several land use classes of which there was insufficient data. This was solved by undertaking a reclassification of the 1995 land use map of Flanders to reduce the number of land use classes. The aim of this reclassification was to simplify the land use input and balance data availability with the detail required of spatially distributed modelling, and to merge very small land uses into similar categories. Determination of which land uses to merge together was undertaken in conjunction with the Ecosystem Management Research Group of the University of Antwerp, who have vast field experience in the Grote Nete catchment. The land uses were reclassified from an initial 20 land use types into the following eight categories: built-up areas (23.5%), bare soil (0.6%), grassland (20.8%), maize (35.7%), pine forest (3.1%), leaf forest (14.7%), wetlands (0.3%) and open water bodies (1.3%). Each land use had an associated user-defined vegetation development file, which contains information on the annual growth cycle, and progression of the Leaf Area Index (LAI) and crop coefficient ( $K_c$ ) values.

#### Model performance evaluation

*Statistical analysis.* A multi-criteria modelling protocol involving both the split-sample approach and a graphical approach using validation plots was employed to test the model during the calibration and validation stages. Hourly river discharge data was used, with a calibration period from 1986–1988 and validation from 1990–1995. Both the measured ( $Q_m$ ) and simulated ( $Q_s$ ) river discharge series were subjected to standard exploratory data analysis to describe the performance of the model by use of three traditional summary statistics, namely the mean square error (MSE), the coefficient of determination ( $R^2$ ) and the efficiency coefficient (EF). The MSE is a measure that considered the average random discrepancy between  $Q_m$  and  $Q_s$ . It is defined as

$$\text{MSE} = \sum_{i=1}^n \frac{[Q_m(i) - Q_s(i)]^2}{n} \quad (12)$$

where  $i$  is the number of observations (1,  $n$ ). The Box–Cox transformation (Bandy and Willems 2000) was applied to both  $Q_m$  and  $Q_s$  in the determination of the MSE, and was defined with a calibration parameter,  $\lambda$ , as

$$\text{BC}(Q_i) = \frac{Q_i^\lambda - 1}{\lambda} \quad (13)$$

The Box–Cox transformation was used because classical sampling theory assumes homoscedasticity, i.e. that the variances of the sampled elements are the same. One of the challenges of rainfall–runoff modelling is that the residual variance is not constant but rather increases with increasing discharge and therefore the assumption of homoscedasticity is invalid (Box and Cox 1964; Sorooshian and Dracup 1980; Chapman 1991; Beven 2000; Boyle et al. 2000). This problem is exaggerated for coefficients like the MSE and EF which have square error terms in their equations. To overcome this limitation, two main approaches have been proposed. The first involves variations to the mathematical expressions of the coefficients (Legates and McCabe 1999; Madsen 2000, 2003), while the second involves transformation of the variables of interest (Kelly and Krzysztofowicz 1997; Kokkonen and Jakeman 2001; Moran 1970). The Box–Cox transformation is an example of the latter. The value of  $\lambda$  for the Grote Nete catchment was previously determined as 0.25 (Rubarenzya et al.

2005b). The EF of Nash and Sutcliffe (Nash and Sutcliffe 1970) was adopted. This is a dimensionless and scaled version of the MSE defined as

$$EF = \left[ 1 - \frac{\sum_{i=1}^n [Q_m(i) - Q_s(i)]^2}{\sum_{i=1}^n [Q_m(i) - \overline{Q_m}]^2} \right] = \left( 1 - \frac{\text{MSE}}{S_m^2} \right) \quad (14)$$

where  $\overline{Q_m}$  and  $S_m$  are the mean and variance of the modelled river discharge series, respectively. The final criterion was the dimensionless coefficient of determination  $R^2$ , defined as

$$R^2 = \frac{\sum_{i=1}^n (Q_{m,i} - \overline{Q_m})^* (Q_{s,i} - \overline{Q_s})}{\sqrt{\sum_{i=1}^n (Q_{m,i} - \overline{Q_m})^2} \sqrt{\sum_{i=1}^n (Q_{s,i} - \overline{Q_s})^2}} \quad (15)$$

The model development objectives were to obtain EF and  $R^2$  greater than 0.7, and MSE less than 0.1.

*Statistical time series processing.* An additional evaluation criterion in the form of statistical time series processing catered for the possible presence of serial dependence, which often occurs in model residuals when series of observations are used. Serial dependence increases with decreasing time steps of the series. It also depends on the flow magnitude (Willems 2005). The serial dependence in high flows is most significant at small time scales, for instance, hourly time steps or time steps less than the recession constant of overland flow. In addition, serial dependence in low flows is more significant than in high flows because low flows have a longer recession constant than high flows. Serial dependence was addressed by extracting nearly independent observations from the flow series through hydrograph separation. A peak over threshold (POT) analysis was performed to split the river discharge series into (nearly independent hydrograph) periods. Discharge peaks were then selected from quick flow hydrographs, while least flow values were selected from low flow periods. Following the POT analysis, the following plots were then derived and used to perform a graphical analysis of the model:

1. Simulated versus measured discharge maxima during (nearly independent) quick flow hydrograph periods.
2. Simulated versus measured discharge minima during (nearly independent) base flow or slow flow hydrograph periods.
3. Cumulative flow volumes.
4. High flow extreme value statistics.
5. Low flow extreme value statistics.
6. Discharge time series, with and without log-scale for the discharge.

It was from this analysis that independent points for use in model performance evaluation were extracted from both the measured and the simulated discharge hydrographs.

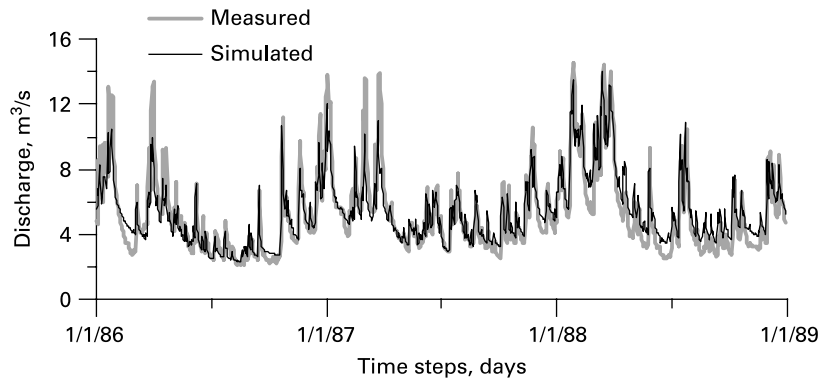
## Results and discussion

An acceptable parameter set was obtained for which all three statistical criteria were met over both the calibration and the validation periods. The MSE was less than  $0.10 \text{ (m}^3/\text{s)}^2$ , and the EF and  $R^2$  coefficients were greater than 0.7 (Table 3). The statistical analyses revealed better model performance during the validation period as compared to the calibration period.

Plots of the measured and simulated hydrographs (Figure 5) revealed an identical trend between the two for the final model parameter set. The analyses performed with peak values extracted by the POT analysis were not influenced by possible time phase shifts between

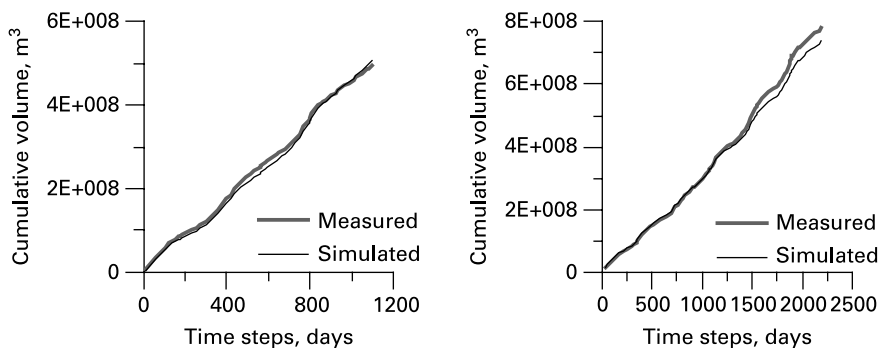
**Table 3** MSE, EF coefficient, and coefficient of determination results

	MSE (m <sup>3</sup> /s) <sup>2</sup>	EF	R <sup>2</sup>
Calibration	0.08	0.75	0.87
Validation	0.08	0.70	0.90

**Figure 5** Detail of measured and simulated stream discharge hydrographs at Varendonk over the calibration period

measured and simulated discharge hydrographs. This was particularly advantageous given that the river discharge series had a small time step (hourly), and it was possible for small time shifts to occur in the model simulation results due to, for instance, the locations of raingauges relative to rainfall fronts within the catchment.

Figures 6, 7 and 8 show some of the plots used in graphical evaluation of the model, the latter two of which were used to test how well the model was able to simulate peak high and low flows. Figure 9 shows an analysis of the performance of the model in representing extreme low values during the calibration and validation periods, respectively. To obtain these extreme low flow values, a POT analysis was carried out on the inverse of the discharge values. Analysis of the performance of individual extreme low flows was performed to assess how well the model is simulating low extremes. In addition, the comparison plots for discharge minima for both the calibration and validation periods (Figure 8) showed points oscillating close to the bisector. The scatter of points about the bisector was less during model validation than during calibration. This indicates that the validation period was better

**Figure 6** Cumulative volume at Varendonk during model calibration (left) and validation (right)

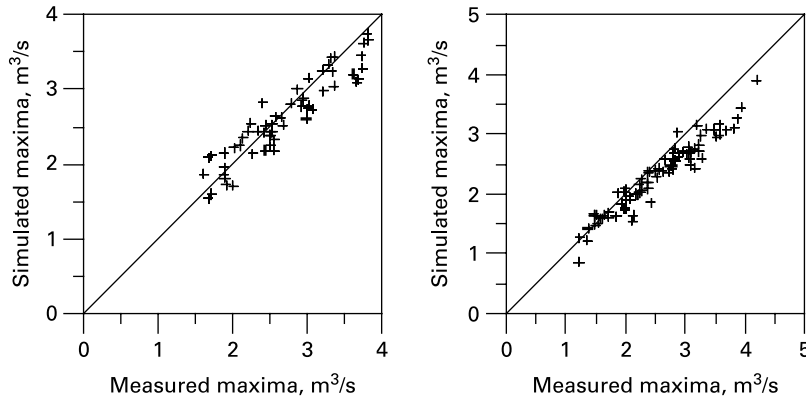


**Figure 7** Comparison plots of discharge maxima from Varendonk (after Box–Cox transformation) during model calibration (left) and validation (right) periods

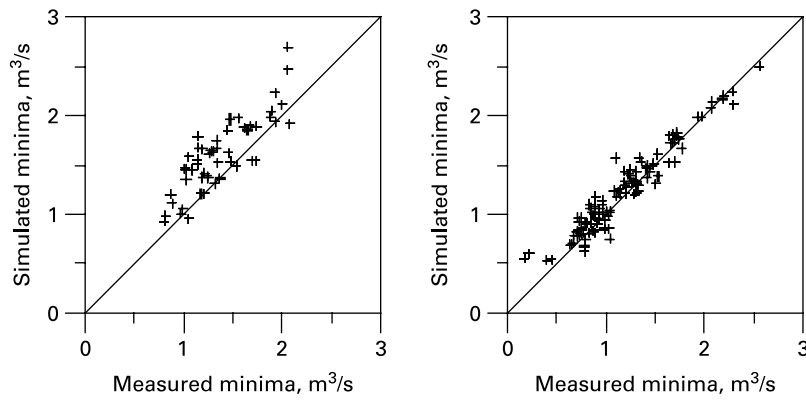


**Figure 8** Comparison plots of discharge minima from Varendonk (after Box–Cox transformation) during model calibration (left) and validation (right) periods

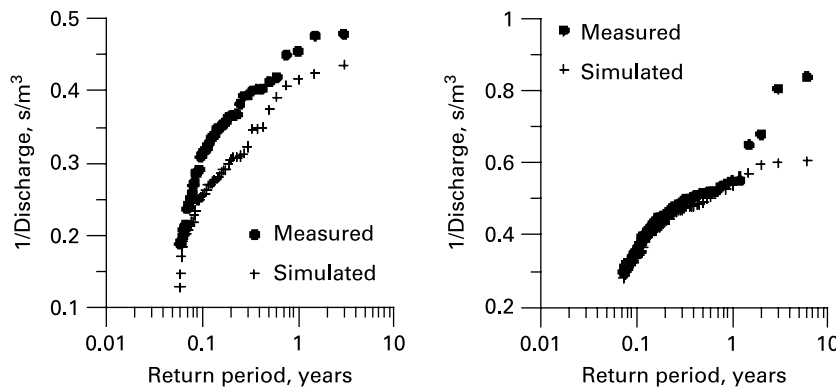


**Figure 9** Comparison plot of extreme low discharge events recorded during the calibration (left) and validation (right) periods at Varendonk

simulated than the calibration period. [Figure 10](#) shows an analysis of the performance of the model in representing extreme high values. The extreme high flow values were obtained from a POT analysis carried out on the discharge values. Here, analysis of the performance of individual extreme high flows was performed, firstly, to rule out any possibility of

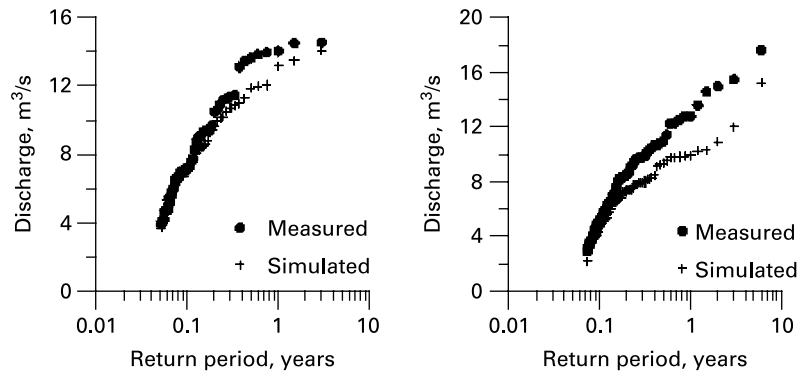


**Figure 10** Comparison plot of extreme high discharge events recorded during the calibration (left) and validation periods (right) at Varendonk

rejecting the model as a consequence of a possible shift (backwards or forward) in the output hydrograph when compared to the measured hydrograph. Secondly, to assess how well the model is simulating high extremes. Studying [Figures 7 and 10](#) leads to the conclusion that there is good agreement between measured and simulated values. It was observed that the scatter of points about the bisector was good for both the model validation and calibration. From the plot of cumulative volumes ([Figure 6](#)) it is concluded that the total flow volume was being well simulated by the model. Generally, the plots of peak flows revealed good overall simulations. [Figure 7](#) showed a good estimation of the peak high flows (see [Figure 5](#)), while [Figure 8](#) showed that the peak low flows were being overestimated during the calibration period. In both cases, the points were all close to the bisectors.

Over 20% of the catchment area consists of urban settlements, with combined sewer networks carrying stormwater (and domestic sewerage) across sub-catchments and quickly into the collecting streams. Rough estimates put the percentage of overland flow from urban drainage at 30–60%. In addition, sewers import additional flow from urban areas outside the model domain. This flow across the boundary could not be readily estimated, and is not included in the model. Although a conceptual drainage component was included in the development of the site-specific model for this catchment, it did little to explicitly represent flow from urban catchments, especially the rapid concentration over sub-catchments by means of long sewer networks. This may be the main factor contributing to the depressed high flow peaks ([Figure 7](#)).

Finally, to further investigate an underestimation of discharge that was observed at Varendonk towards the end of the validation period ([Figure 6](#)), a plot was made of extreme high discharges and discharge ratio,  $r$  (ratio of measured to simulated discharge), for the periods 1986–1987, 1990–1991, 1992–1993 and 1994–1995 ([Figure 11](#)). The period

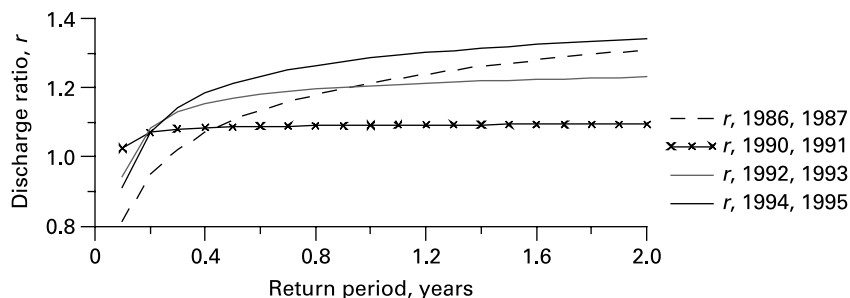


**Figure 11** Discharge ratio (measured/simulated discharge) plotted against the return period at Varendonk (2-year periods between 1986 and 1995)

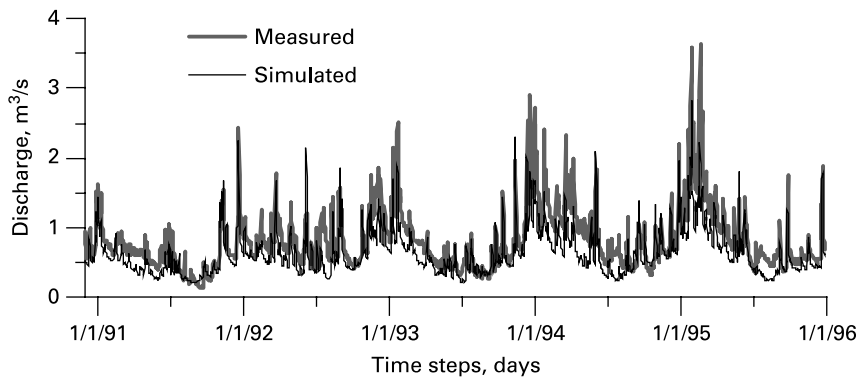


**Figure 12** Detail of measured and simulated stream discharge hydrographs at Vorst over the validation period

1987–1989 was excluded because it had a period with erroneous data. From the plot, a drop is observed in the discharge ratio,  $r$ , in moving from 1986–1987 to 1990–1991, after which a progressive increase is observed from 1990–1991 through to 1994–1995. The results of this analysis indicate the absence of a trend in the discharge at Varendonk since the discharge ratio is shown to both reduce and increase during this validation period. Comparable simulation results as at Varendonk were obtained for the limnigraphic station at Vorst (Figure 12).

## Conclusions

This paper has outlined the development of a physically based, fully distributed model as was realised for the Grote Nete catchment using MIKE SHE. This paper highlighted the various stages of model development from conceptualisation of the model and the underlying mathematical representation of hydrological processes, through the model set-up phase, and finally to the calibration and validation of the model. Each of the hydrological processes was represented at different levels of spatial distribution and complexity, dependent upon the availability of field data. The multi-dimensional Grote Nete catchment model was built to include a three-dimensional solution for saturated–unsaturated flow in the subsurface, and one- and two-dimensional solutions for surface water flow, all of which solutions were tightly coupled and linked through time-lags. The two-dimensional solution simulated overland rainfall–runoff processes, while the one-dimensional solutions simulated channel flow. This is an example of the development of a site-specific model. Over both the calibration and the validation periods, the MSE of river discharge was less than  $0.10 \text{ (m}^3/\text{s)}^2$ , and the EF and  $R^2$  coefficients were greater than 0.7. Graphical comparison of measured and simulated river discharge series using seven evaluation plots showed good model performance during both calibration and validation periods. An acceptable parameter set would be determined.

The Grote Nete catchment model is being applied for conjunctive land and water management evaluations, specifically studying the potential hydrological consequences on river discharges of anthropogenic perturbations in the form of river valley rewetting. In the research, output from a Spatial Analysis tool (SPAN) (Staes and Meire 2006) is integrated into the model. The combined modelling platform is then used for the integrated assessment of river valley rewetting potential, addressing the hydrological, social and ecological aspects of the process.

## Acknowledgements

This research was funded by the Interuniversity Programme in Water Resources Engineering (IUPWARE). The authors appreciate the constructive comments and suggestions of the anonymous reviewers of this paper.

## References

- Allen, G.R., Pereira, L.S., Raes, D. and Martin, S. (1998). *Crop Evapotranspiration — Guidelines for Computing Crop Water Requirements*. Rep. No. Paper 56. Food and Agriculture Organisation, Rome, Italy.
- Bandy, J. and Willems, P. (2000). Towards a more physically-based calibration of lumped conceptual rainfall-runoff models. *Hydroinformatics 2000*, CD-ROM proceedings, Iowa, 12.
- Batelaan, O. (2006). Phreatology. *Characterising Groundwater Recharge and Discharge Using Remote Sensing, GIS, Ecology, Hydrochemistry, and Groundwater Modelling*. PhD thesis. Vrije Universiteit Brussel.
- Beven, K.J. (1985). Distributed modelling. In M.G. Anderson and T.P. Burt (Eds.), *Hydrological Forecasting*, Wiley, Chichester, pp. 405–435.
- Beven, K.J. (1993). Prophecy, reality and uncertainty in distributed hydrological modelling. *Adv. Wat. Res.*, **16**, 41–51.
- Beven, K.J. (1996). A discussion of distributed modelling. In J.C. Refsgaard and M.B. Abbott (Eds.), *Distributed Hydrological Modelling*, Kluwer, Dordrecht, pp. 255–278.
- Beven, K.J. (2000). Uniqueness of place and process representations in hydrological modelling. *Hydrol. Earth Syst. Sci.*, **4**(2), 203–213.
- Beven, K.J. (2001). How far can we go in distributed hydrological modelling? *Hydrol. Earth Syst. Sci.*, **5**(1), 1–12.
- Blöschl, G. (2001). Scaling in hydrology. *Hydrol. Process (HP Today)*, **15**, 709–711.
- Boyle, D.P., Gupta, H.V. and Sorooshian, S. (2000). Towards improved calibration of hydrological models: combining the strength of manual and automatic methods. *Wat. Res. Res.*, **36**(12), 3663–3674.
- Carpenter, T.M. and Georgakakos, K.P. (2004). Impacts of parametric and radar rainfall uncertainty on the ensemble streamflow simulations of a distributed hydrological model. *J. Hydrol.*, **298**(1–4), 202–221.
- Chapman, T. (1991). Comment on “Evaluation of automated techniques for base flow and recession analysis” by Nathan, R.J. and McMahon, T.A. *Wat. Res. Res.*, **27**(7), 1783–1784.
- Graham, D.N. and Butts, M.B. (2006). Flexible integrated watershed modeling with MIKE SHE. In V.P. Singh and D.K. Frevert (Eds.), *Watershed Models*, Taylor and Francis/CRC Press, Boca Raton, FL, pp. 245–272.
- Havno, K., Madsen, M.N. and Dorge, J. (1995). MIKE 11 - A generalised river modelling package. In V.P. Singh (Ed.), *Computer Models of Watershed Hydrology*, Water Resources Publications, CO, pp. 809–846.
- Jungwirth, M., Muhar, S. and Schmutz, S. (2002). Re-establishing and assessing ecological integrity in riverine landscapes. *Freshwater Biol.*, **47**, 867–887.
- Kelly, K.S. and Krzysztofowicz, R. (1997). A bivariate meta-Gaussian density for use in hydrology. *Stochast. Hydrol. Hydraul.*, **11**, 17–31.
- Kokkonen, T.S. and Jakeman, A.J. (2001). A comparison of metric and conceptual approaches in rainfall-runoff modeling and its implications. *Wat. Res. Res.*, **37**(9), 2345–2352.
- Kristensen, K.J. and Jensen, S.E. (1975). A model for estimating actual evapotranspiration from potential transpiration. *Nordic Hydrol.*, **6**, 70–88.
- Kusler, J.A. and Kentula, M.E. (1990). *Wetland Creation and Restoration: The Status of The Science*, Island Press, Washington, DC.
- Legates, D.R. and McCabe, G.J. (1999). Evaluating the use of “goodness-of-fit” measures in hydrologic and hydroclimate model validation. *Wat. Res. Res.*, **35**(1), 233–241.
- Madsen, H. (2000). Automatic calibration of a conceptual rainfall-runoff model using multiple objectives. *J. Hydrol.*, **235**, 276–288.
- Madsen, H. (2003). Parameter estimation in distributed hydrological catchment modeling using automatic calibration with multiple objectives. *Adv. Wat. Res.*, **26**(2), 205–216.
- Michaud, J. and Sorooshian, S. (1994). Comparison of simple versus complex distributed runoff models on a mid-sized semiarid watershed. *Wat. Res. Res.*, **30**(3), 593–605.
- Mitsch, W.J. (1993). Ecological engineering – a cooperative role with the planetary life-support systems. *Environ. Sci. Tech.*, **27**, 438–445.
- Mitsch, W.J. (1998). Ecological engineering – the seven year itch. *Ecol. Engng.*, **10**, 119–138.



- Mitsch, W.J., Lefeuve, J.C. and Bouchard, V. (2002). Ecological engineering applied to river and wetland restoration. *Ecol. Engng.*, **18**(5), 529–541.
- Mitsch, W.J. and Wilson, R.F. (1996). Improving the success of wetland creation and restoration with know-how, time and self-design. *J. Appl. Ecol.*, **6**, 77–83.
- Moran, P.A.P. (1970). Simulation and evaluation of complex water system operations. *Wat. Res. Res.*, **6**, 1737–1742.
- Nash, J.E. and Sutcliffe, I.V. (1970). River flow forecasting through conceptual models. *J. Hydrol.*, **273**, 282–290.
- Niehoff, D., Fritsch, U. and Bronstert, A. (2002). Land-use impacts on storm-runoff generation: scenarios of land-use change and simulation of hydrological response in a meso-scale catchment in SW Germany. *J. Hydrol.*, **267**(1–2), 80–93.
- Palmer, M.A., Bernhardt, E.S., Allan, J.D., Lake, P.S., Alexander, G., Brooks, S., Carr, J., Clayton, S., Dahm, C.N., Shah, J.F., Galat, D.L., Loss, S.G., Goodwin, P., Hart, D.D., Hassett, B., Jenkinson, R., Kondolf, G.M., Lave, R., Meyer, J.L., O'Donnell, T.K., Pagano, L. and Sudduth, E. (2005). Standards for ecologically successful river restoration. *J. Appl. Ecol.*, **42**, 208–217.
- Pedroli, B., De Blust, G., Van Looy, K. and Van Rooij, S. (2002). Setting targets in strategies for river restoration. *Landscape Ecol.*, **17**(Suppl. 1), 5–18.
- Raes, D., Van Aelst, P. and Wyseure, G. (1986). *ETREF, ETCROP, ETSPLIT, and DEFICIT. A Computer Package for Calculating Crop Water Requirements*, Leuven, Laboratory of Soil and Water Engineering, Katholieke Universiteit Leuven, Belgium.
- Reed, S., Koren, V., Smith, M., Zhang, Z., Moreda, F., Seo, D.J., Arnold, J.G., Bandaragoda, C., Bingeman, A., Bras, R., Butts, M.B., Carpenter, T.M., Cui, Z., Diluzio, M., Georgakakos, K.P., Gaur, A., Guo, J., Gupta, H.V., Hogue, T., Ivanov, V., Khodatalab, N., Lan, L., Liang, X.L.D., Mitchell, K., Peters-Lidard, C., Rodriguez, E., Seglenieks, F., Shamir, E., Tarboton, D., Vieux, B., Vivoni, E. and Woods, R. (2004). Overall distributed model intercomparison project results. *J. Hydrol.*, **298**, 27–60.
- Refsgaard, J.C. and Knudsen, J. (1996). Operational validation and intercomparison of different types of hydrological models. *Wat. Res. Res.*, **32**(7), 2189–2202.
- Refsgaard, J.C. and Storm, B. (1995). MIKE SHE. In V.P. Singh (Ed.), *Computer Models for Watershed Hydrology*, Water Resources Publications, Highland Ranch, CO, pp. 809–846.
- Reggiani, P., Hassanizadeh, S.M., Sivapalan, M. and Gray, W.G. (1999). A unifying framework for watershed thermodynamics: constitutive relationships. *Adv. Wat. Res.*, **23**, 15–39.
- Reggiani, P., Sivapalan, M. and Hassanizadeh, S.M. (1998). A unifying framework for watershed thermodynamics: balance equations for mass, momentum, energy and entropy and the second law of thermodynamics. *Adv. Wat. Res.*, **23**, 15–40.
- Reggiani, P., Sivapalan, M. and Hassanizadeh, S.M. (2000). Conservation equations governing hillslope response: exploring the physical basis of water balance. *Wat. Res. Res.*, **16**, 1845–1863.
- Richardson, C.J. (1994). Ecological functions and human values in wetlands: a framework for assessing forestry impacts. *Wetlands*, **14**, 1–9.
- Ripl, W., Hildmann, C., Janssen, T., Gerlach, I., Heller, S. and Ridgill, S. (1995). *Sustainable Redevelopment of a River and its Catchment – The Stör River Project*, IWRB Publication, Slimbridge, UK.
- Rouhani, H. (2004). *Report of Rainfall Input Data: Grote Nete and Grote Laak Catchments*, Laboratory of Hydraulics, Katholieke Universiteit Leuven, Belgium.
- Rubarenzya, M.H., Willems, P., Berlamont, J. and Feyen, J. (2005a). Applying MIKE SHE to define the influence of rewetting on floods in Flanders. In: *Proceedings of the Fourth Inter-Celtic Colloquium on Hydrology and Management of Water Resources, Guimaraes, Portugal*. Available on CD-ROM.
- Rubarenzya, M.H., Willems, P., Berlamont, J. and Feyen, J. (2005b). *Modelling of River Valley Rewetting and Extreme Events in the Nete Catchment (Belgium)*, Taylor & Francis/A.A. Balkema Publishers, Leiden, The Netherlands.
- Rubarenzya, M.H., Willems, P., Feyen, J. and Berlamont, J. (2006). Modeling of soil hydraulic properties and base flow in Flanders. In: *Proceedings of the EWRI World Environmental and Water Resources Congress, Omaha, NB*. The American Society of Civil Engineers.
- Smith, R.E., Goodrich, D.R., Woolhiser, D.A. and Simanton, J.R. (1994). Comments on “Physically-based hydrological modelling Is the concept realistic?” by R.B. Grayson, I.D. Moore and T.A. McMahon. *Wat. Res. Res.*, **30**, 851–854.

- Sorooshian, S. and Dracup, J.A. (1980). Stochastic parameter estimation procedures for hydrologic rainfall-runoff models: correlated and heteroscedastic error cases. *Wat. Res. Res.*, **16**(2), 430–442.
- Staes, J. and Meire, P. (2006). *A Tool for Participatory Land-use Planning and River Basin Management*, International Seminar on Collaborative Planning of Natural Resources Management, Helsinki, Finnish Environment Institute, Finland.
- Todd, J., Brown, E.J.G. and Wells, E. (2003). Ecological design applied. *Ecol. Engng.*, **20**, 421–440.
- Tucciarelli, T. (2003). A new algorithm for a robust solution of the fully dynamic Saint-Venant equations. *J. Hydraul. Res.*, **41**(3), 239–246.
- Vazquez, F.R. (2004). *Report on the Computation of ETo using Data for the Geel Station (Belgium) with Application to the Hydrological Modelling using the MIKE SHE Code*. Rep. No. Internal Report, Laboratory of Hydraulics, Katholieke Uviersiteit Leuven, Leuven, Belgium.
- VLIZ: Flanders Marine Institute (2006). *AMINAL Limnietric or Hydrologic Monitoring Network Non-navigable Waterways*. Available at: <http://www.vliz.be/Vmdcdata/imis2/Dataset.php?show=html&dasis=451>.
- Willems, P. (2000). *Probablistic Immission Modelling of Receiving Surface Waters*. PhD Thesis, Faculty of Engineering, Katholieke Universiteit Leuven, Belgium.
- Willems, P. (2003). *WETSPRO: Water Engineering Time Series PROgramming Tool, Methodology and User's Manual ver.2.0*. Leuven, Katholieke Universiteit Leuven.
- Willems, P. (2005). *Guidance Document for Calibration and Verification of Rainfall-runoff Models*, K.U. Leuven Hydraulics Laboratory, Belgium.
- Willems, P., Vaes, G., De Lannoy, G. and Verhoest, N. (2002). *A Spatial Rainfall Model for Flanders* (in Dutch: Een ruimtelijk neerslagmodel voor Vlaanderen). Rep. No. Study report for the Ministry of the Flemish Community (AMINAL, AWZ, Aquafin), Laboratory of Hydraulics, Katholieke Universiteit Leuven; KMI, Leuven, Belgium.